This is a preprint, the final version is subject to change, of the American Mineralogist (MSA)
Cite as Authors (Year) Title. American Mineralogist, in press.
(DOI will not work until issue is live.) DOI: http://dx.doi.org/10.2138/am-2017-6081

Revision 2

The role of modifier cations in network cation coordination increases with pressure in aluminosilicate glasses and melts from 1 to 3 GPa

Saurav Bista,[1,a)] Jonathan F. Stebbins[1]

[1]Department of Geological Sciences, Stanford University, Stanford, California 94305, USA

[a)]corresponding author, sbista@stanford.edu

This is a preprint, the final version is subject to change, of the American Mineralogist (MSA)
Cite as Authors (Year) Title. American Mineralogist, in press.
(DOI will not work until issue is live.) DOI: http://dx.doi.org/10.2138/am-2017-6081

ABSTRACT

Previous studies have shown that both NBO content and modifier cation field strength play important roles in increasing the network cation coordination with increasing pressure. It has been observed in previous studies that the increase in average Al coordination with pressure in alkali aluminosilicates depends on NBO concentration, where large increases in Al coordination with pressure have been observed for compositions containing significant concentrations of NBO and little or no Al coordination increase observed in glasses containing negligible NBO at pressures ranging from 1 to 3 GPa. Similarly, in NBO rich aluminosilicates and aluminoborosilicates containing different modifier cations, it was reported that the increase in average Al coordination followed a steeper rise with increasing pressure in compositions containing higher field strength modifier. In this study, we look at Ca- and Mg-aluminosilicate glasses across all three compositional regimes (peralkaline, metaluminous and peraluminous) to study the effect of both oxygen speciation and modifier cation field strength on network cation coordination changes with pressure. Our study shows that in Mg aluminosilicate glasses (both peralkaline and metaluminous), the increase in average Al coordination can be quite large and show no significant impact from differences in oxygen speciation (NBO content). In contrast, in Ca-aluminosilicate glasses, the oxygen speciation has a notable impact with the average Al coordination following a steeper rise with increasing pressure in a peralkaline composition and less steep for a metaluminous composition.

INTRODUCTION

The properties of melts and glasses at high pressure are significantly different from those at ambient pressure, and such changes, as well as their structural causes, are important for geological processes as well as technological applications (Striepe et al. 2013; Januchta et al. 2017). In aluminosilicate melts, the changes in aluminum structural environment with increasing pressure have been widely studied through ^{27}Al MAS NMR studies on glasses that are quenched from high temperatures at high pressure and decompressed to ambient pressure (Yarger et al. 1995; Allwardt et al. 2005a; Kelsey et al. 2009b; Lee et al. 2012). Significant coordination increases have been recorded with this approach. Recent studies have also shown, however, that large transient pressure drops may occur during quench from high temperatures in solid-media apparatus, and that resulting data may actually significantly underestimate structural changes (Bista et al. 2015). More accurate recording of the actual quench pressure, and resulting structural changes, can be made in experiments conducted near the glass transition temperature (T_g). Near to T_g, the structure can relax to that of the metastable, supercooled liquid within seconds or minutes, without the need for subsequent substantial cooling to quench in the structure, which can be accompanied by significant pressure drop caused by thermal contraction.

It is important to note that in-situ experiments at high pressure and temperature would be ideal to completely characterize the pressure effects on structure, but as yet are not feasible to observe the detailed changes measurable by NMR on recovered, decompressed glasses. In-

situ Raman spectroscopic studies of silicate melts and glasses at high pressure have shown some evidence that the structure of decompressed glasses can be different from those at high pressure (Wolf et al. 1990; Farber and Williams 1996), particularly at very high pressures where all network cations have increased coordination numbers. Our previous studies of the effect of decompression rates on recovered structural changes from high pressure (Allwardt et al. 2004, 2005b) also point to possible effect of decompression on ex-situ analysis of the recovered glass. Some aspects of structural relaxation may occur more readily upon decompression (e.g. elastic compression of oxygens around weakly-bonded modifier cations and distortion of network cation polyhedra) while others might be expected to change more slowly on decompression at ambient T (e.g. those involving breaking strong network bonds such as Si, Al, and B coordination). It is clear that in the range of pressure and densification studied here, large changes in network cation coordination, network bond angle distribution, and even some changes in modifier cation coordination are retained (Kelsey et al. 2009b), which record major effects of composition and which are correlated with measured, recovered density increases. In one unique study (Malfait et al. 2014), measurements of elastic constants and in-situ densities of aluminosilicate liquids and glasses in the 3.5 GPa range suggested that inelastic loss in densification during decompression was not large, suggesting also that structural changes were minor. Future in-situ structural studies may be able to more clearly determine what structural changes take place during decompression, and it may be that results on quenched, decompressed glasses represent only minimum estimates of changes present at high pressure and the glass transition temperature.

In any case, correlating observed structural changes with observed, recovered density changes, as done in this and other recent studies, does give a robust picture of the role of network structure, and effects of composition, on measured density increases that must be an important part of those which take place in magmas in the Earth's lower crust and upper mantle. The pressures and temperatures at which such density increases are actually obtained will of course become more accurately known with further in-situ melt density measurements (Malfait et al. 2014)

All data on quenched, decompressed glasses suggest that pressure-induced changes in aluminum coordination changes, as well as other structural variables, are strongly dependent on the composition. Studies done on alkali aluminosilicate glasses with varying contents of NBO have shown that the rate of increase in Al coordination with pressure is much reduced in more polymerized melts (low NBO, e.g. jadeite composition) (Lee et al. 2004, 2012; Bista et al. 2015), confirming an important role of NBO in one common mechanism for such changes. Another critical compositional variable is the field strength of the modifier cation, defined as the ratio of the formal charge to the square of the average cation-oxygen distance (Brown et al. 1995). Contents of highly coordinated aluminum species (^{V}Al and ^{VI}Al) are now well-known to increase with modifier field strength (e.g. $K^{1+} < Na^{1+} < Ca^{2+} < Mg^{2+} < La^{3+}$) in both ambient and high pressure glasses (Allwardt et al. 2005a; Neuville et al. 2008; Kelsey et al. 2009a; Bista et al. 2016). However, knowledge of the role of NBO and modifier cation field strength on network cation coordination change are derived from a fairly limited range of compositions, primarily peralkaline and metaluminous alkali aluminosilicates and NBO-rich systems with higher field strength modifiers (Lee et al. 2004, 2012; Allwardt et al. 2005a; Kelsey et al. 2009a; Gaudio et

al. 2015). While Na aluminosilicate glasses containing little to no NBO have only small increases in aluminum coordination in the pressure range from 1-3 GPa, the same cannot be said for peraluminous and metaluminous aluminosilicate glasses containing higher field strength modifiers Ca and Mg, whose effects are much less known despite their importance in mafic and ultramafic magmas.

In this study, we look at Ca- and Mg-aluminosilicate glasses in peralkaline earth, meta- and peraluminous compositions to study pressure induced aluminum coordination changes at 1.5 to 3 GPa, which is highly relevant to the pressure range at which most magmas form in the mantle of the modern Earth. The high pressure experiments were done by quenching supercooled liquids from temperatures near to T_g, which not only greatly reduces problems with pressure drop during quench, but allows study of Mg-rich compositions whose high liquidus temperatures and poor glass-forming abilities can be problematical for super-liquidus experiments (Allwardt et al. 2005). Because pressure can affect T_g (Bagdassarov et al. 2004), this approach necessitates runs at several different temperatures to ensure full structural relaxation at pressure. Density measurements on recovered glasses complement the data from spectroscopy and help to define the importance of observed structural changes to overall compaction at high pressure. We complement ^{27}Al NMR data with studies of ^{17}O and ^{29}Si spectra of a number of high pressure calcium aluminosilicate glasses, where effects of increasing Al coordination can be quite marked.

Aluminum coordination changes are readily observable at 1.5 to 3 GPa, and do mark important effects of composition on the response of the melt structure to pressure that are likely to be important for physical properties and thermodynamic activities (Stebbins 2016).

126 However, in most compositions it is clear that Al coordination increases by themselves can
127 account for only a small part of the overall melt density increase (Allwardt et al. 2005).

128

129 **EXPERIMENTAL METHODS AND DATA ANALYSES**

130 Ca- and Mg- aluminosilicate glasses of different modifier (CaO or MgO) to alumina
131 (Al_2O_3) ratios were chosen to study the effect of the type of modifier and the oxygen speciation
132 on pressure induced structural changes, at a constant 60 mole % silica. Three different
133 compositions of Ca-aluminosilicate glasses ("peralkaline earth", $CaO>Al_2O_3$; metaluminous,
134 $CaO\approx Al_2O_3$ and peraluminous, $CaO<Al_2O_3$) and two different compositions of Mg-
135 aluminosilicate glasses ("peralkaline earth" and metaluminous) were studied. 3 to 6 grams
136 batches were initially melted at ambient pressure using reagent grade $CaCO_3$, MgO, Al_2O_3 and
137 SiO_2 with 0.1 wt% cobalt oxide added to speed the spin lattice relaxation rates. The
138 compositions were analyzed using EPMA and were close to nominal (Table 1). Two ^{17}O-enriched
139 Ca-aluminosilicate glasses from a previous study of oxygen speciation (Thompson and Stebbins
140 2011) were also selected for high pressure experiments here. The T_g (onset temperature) of
141 each starting glass was measured using a Netzsch 404F3 differential scanning calorimeter (DSC)
142 at a heating rate of 10 K/min and is included in Table 2. High pressure samples were prepared
143 from starting glasses in 100 to 150 mg batches in sealed Pt tubes as described in our previous
144 studies (Bista et al. 2015, 2016). Samples were held at high temperature and pressure for 1.5
145 hr. Structural relaxation was confirmed for the 3 GPa samples by conducting experiments at

multiple temperatures near to the expected T_g and subsequent ^{27}Al MAS NMR and density measurements on recovered glasses.

^{27}Al, ^{29}Si and ^{17}O MAS NMR data were obtained using Varian/Chemagnetics "T3" probes and Varian 18.8 T (208.4 MHz for ^{27}Al), 9.4 T (79.4 MHz for ^{29}Si) and 14.1 T (81.34 MHz for ^{17}O) spectrometers. Samples were spun at 20 kHz in 3.2 mm zirconia rotors and frequencies are reported relative to 0.1 M aqueous $Al(NO_3)_3$ for ^{27}Al, tetramethylsilane for ^{29}Si and ^{17}O-enriched H_2O for ^{17}O, each set at 0 ppm. Spectra were collected using single pulse acquisition with pulse widths corresponding to 30° radio frequency tip angles (solid). Pulse delays of 0.1 s were used for ^{27}Al, a range of pulse delays from 10 to 30 s for ^{29}Si and 1 s for ^{17}O. No differential relaxation for different components of the spectra was observed. The areas of the three peaks in the ^{27}Al spectra, corresponding to ^{IV}Al, ^{V}Al and ^{VI}Al, were quantified by fitting the individual peaks using the Czjzek distribution of quadrupolar coupling constants (C_Q) in DMFit software (Massiot et al. 2002). For consistency with our new NMR data, spectra collected with the same instrument and previously published (Allwardt et al. 2005a, 2007) were refitted with identical procedures. For ^{17}O and ^{29}Si spectra, only qualitative comparisons of pressure induced-changes were made, as these did not have resolved components.

Density measurement were done using the sink/float technique with a diiodomethane/acetone solution (Table 2) (Bista et al. 2015). For each glass fragment of a few mg, acetone was added to diiodomethane until it sank; eventually the fragment would re-float after some acetone had evaporated from the solution. Proportions of the two liquids were measured by weight and were used to calculate the density of the glass. A control sample of pure diiodomethane was also maintained for recording the evaporation rate of this much less

168 volatile component and a correction was applied. This method is especially precise for
169 determining pressure-induced relative changes in density of small glass fragments.

170

171 **RESULTS**

172 **^{27}Al MAS NMR**

173 Figures 1a, b, c, d show the 18.8 Tesla ^{27}Al MAS NMR spectra of CAS 2020, CAS1525,
174 MAS2020 and MAS3010 respectively, recovered from various pressures. Three peaks in the
175 spectra can be uniquely assigned to aluminum with fourfold-, fivefold- and sixfold- coordination
176 (^{IV}Al, ^{V}Al, ^{VI}Al). The fraction of each species can be quantified by fitting each peak with
177 appropriate lineshapes (Massiot et al. 2002) and calculating the relative areas (Table 2). Each
178 peak is asymmetric due to quadrupolar effect.

179 Both experimental and molecular dynamics studies of silicate melts show the viscosity
180 and glass transition behavior with pressure are compositionally dependent (Gaudio and
181 Behrens 2009; McMillan and Wilding 2009; Wondraczek et al. 2009; Karki et al. 2011; Gaudio et
182 al. 2015), where polymerized silicate melts show anomalous viscosity decreases in relatively
183 low pressure regimes (<5 GPa). Therefore, for studies of pressure effects on supercooled liquid
184 structure made near to T_g, it is important to test a range of run temperatures to confirm the
185 completion of the structural relaxation when T_g may vary significantly from its ambient pressure
186 value, as we have done in previous study (Bista et al. 2015). Figures 2a and b compare ^{27}Al MAS
187 NMR spectra for CAS 1525, CAS3010, MAS3010 and MAS2020 recovered from 3 GPa and
188 various temperatures. Spectra for both CAS3010 and CAS1525 glasses recovered from 3 GPa

189 and two different temperatures (810 °C, 850 °C for CAS 3010, and 845 °C, 865 °C for CAS 1525)
190 are very similar (Fig 2a) and the average aluminum coordination for the two different
191 temperatures are also same (4.43 for CAS 3010 and 4.40 for CAS1525) (Table 2) after
192 quantitation of the spectra, suggesting that the samples are most probably structurally relaxed.
193 We report data from only one temperature (810 ˚C) for CAS2020 recovered from 3 GPa because
194 of crystallization at higher temperature. In Figure 2b, for both MAS3010 and MAS2020 the
195 glasses recovered from 835 ˚C have larger fractions of high coordinated aluminum (^{V}Al and ^{VI}Al)
196 (average aluminum coordination: 4.51 for MAS 3010 and 4.53 for MAS 2020) than do samples
197 from slightly lower or higher temperatures. For MAS3010, samples recovered from 810 ˚C and
198 855 ˚C have slightly less high coordinated aluminum (average aluminum coordination: 4.46 for
199 810 °C and 4.39 for 855 °C) as can be seen both in the overlaid spectra and from the results of
200 fitting shown (Table 2). Similarly, for MAS2020, the samples recovered from 810 ˚C and 850 ˚C
201 have reduced high coordinated aluminum (average aluminum coordination: 4.43 for 810 °C and
202 4.50 for 850 °C). As discussed below, these findings suggest incomplete relaxation at the lowest
203 of the three temperatures, and a slight pressure drop during quench from the highest
204 temperature explored. For further calculations and data plots, only samples that contained the
205 highest fraction of high coordinated aluminum at each pressure are considered.

206 In Figures 1a, b and Table 2 for the Ca-aluminosilicate glasses, the changes in ^{27}Al
207 spectra with pressure are smaller for CAS2020 than for CAS1525. Upon quantification of these
208 spectra and taking values from our previous study (Bista et al. 2015) for CAS 3010, the increases
209 in Al coordination are larger for the peralkaline earth composition (average aluminum
210 coordination: 4.03 at 1 bar to 4.43 at 3 GPa), relatively smaller in metaluminous glass (average

aluminum coordination: 4.04 at 1 bar to 4.23 at 3 GPa), and again larger for the peraluminous glass (average aluminum coordination: 4.10 at 1 bar to 4.40 at 3 GPa). Figure 3 shows the plot of average Al coordination number versus pressure, and clearly shows the different trends with composition for the CAS glasses. In contrast, both of the Mg-aluminosilicate glasses follow very similar trends in average Al coordination with pressure (average aluminum coordination: 4.51 for MAS 3010 and 4.53 for MAS 2020, both recovered from 3 GPa and 835 °C). Also, at 3 GPa the average Al coordination numbers for the Mg-aluminosilicate glasses are larger than those for the Ca-aluminosilicate glasses.

Density

Glasses recovered from the high pressure experiments were 2 to 13% denser than ambient pressure samples (Table 2). Figure 4 plots the average Al coordination versus relative densification. The MAS3010 glasses recovered from 3 GPa and three different temperatures for the relaxation study have measurably different densities, where the sample quenched from 835 ˚C is denser compared to samples recovered from 810 and 855 ˚C (11.8, 10.8 and 10.5% densification for 835, 810 and 855 ˚C respectively). Similarly, for MAS2020, the sample recovered from 835 ˚C is denser than samples from 810 and 850 ˚C (12.8, 12 and 12.6% densification for 835, 810 and 850 ˚C respectively). These observations are in agreement with our observation of the largest concentration of high coordinated aluminum seen at 835 ˚C for both Mg-aluminosilicate compositions. For CAS3010, the 810 ˚C sample is slightly less dense

231 compared to that from 850˚C (7.4% for 810 ˚C and 8.2% for 850 ˚C), in spite of nearly identical
232 Al coordination. This anomaly is discussed below.

233

234 **^{29}Si MAS NMR**

235 Figure 5 compares the ^{29}Si MAS NMR spectra of glasses recovered from 1 bar and 3 GPa
236 (for CAS1525, CAS2020, CAS3010 and jadeite) and 2 GPa (for NS3). Only the frequency range for
237 ^{IV}Si is shown: no signal from higher coordinated Si was detectable in these samples and was not
238 expected for these pressures and compositions. As is typical for aluminosilicate glasses,
239 contributions to the spectra for Si species with varying numbers of bridging oxygens (Q^n) or Al
240 first neighbors were unresolved and we did not attempt a model-dependent fit of the data. The
241 NMR peak for each glass shifts to higher frequency (to the left as plotted) with increasing
242 pressure, as seen in previous studies of silicate glasses (Xue et al. 1991; Kelsey et al. 2009b).
243 This shift is largest for CAS1525 with the highest concentration of aluminum and smallest for
244 CAS3010.

245 Also shown are data for jadeite ($NaAlSi_2O_6$) composition glass from 1 bar and 3 GPa.
246 There are no obvious pressure-induced changes in the spectra. In our previous study (Bista et
247 al. 2015), we estimated the percentage of ^{V}Al in this 3 GPa glass to be no more than 0.5 %,
248 despite a recovered densification of 6.7%. ^{29}Si spectra for a $Na_2Si_3O_7$ (NS3) glass containing 0.5
249 mol % alumina from 1 bar and 2 GPa (Bista et al. 2015) are also included in Figure 5. Here, there
250 is partial resolution of signals for Q^3 and Q^4 groups as is typical for alkali silicate glasses, but
251 changes in speciation reported from higher pressure experiments (Xue et al. 1988, 1991; Kelsey

et al. 2009b) are not obvious at these lower pressures. This 2 GPa glass does contain about 35% total high coordinated Al with a 5% recovered densification, but its Al content is low enough to limit the effects of these changes on ^{29}Si spectra.

^{17}O MAS NMR

Figure 6 compares the ^{17}O MAS NMR spectra for the CAS1525 and CAS2020 glasses from 1 bar and 3 GPa. Both are dominated by a single, asymmetric peak with overlapping contributions from oxygens bonded only to Si and/or Al. The latter glass from 1 bar also shows a small peak at about 110 ppm from a few % NBO as described previously (Stebbins et al. 2008; Thompson and Stebbins 2011). For both compositions there are significant shifts of the main peak to higher frequency (left) in the high pressure glasses, which develop important contents of high-coordinated Al (Table 2). This shift, however, obscures the NBO region for the CAS2020 glass and makes any small changes in this area difficult to ascertain, unlike the NBO reductions that have been seen in high pressure CAS glasses with much higher NBO contents (Lee 2003, 2004; Allwardt et al. 2005b)

Hard sphere model calculations

Liquids can respond to pressure readily through configurational changes. Glasses can capture such pressure effects on the structures of supercooled liquids as they are quenched through the glass transition temperature. With increasing pressure, the configurational changes

occur to reduce the volume, and the relation between these structural changes and volume can be compared using metrics such as packing fraction, which is normalized to allow comparison between glasses of wide ranges of composition (Bista et al. 2009; Wang et al. 2014; Zeidler et al. 2014).

In oxide glasses, the response of oxygen to compression becomes important because of its adaptability in size with respect to the coordination environment. Oxygen packing has been used in recent studies (Wang et al. 2014; Zeidler et al. 2014) to help understand trends in structural changes. The radius of the oxygen anion used in this approach varies according to the type and coordination number of the cations with which it is associated. Values for the oxygen anion radius (r_{ox}) associated with various coordination of network cation are based on Zeidler et al. (2014) (1.306 Å for ^{IV}Si, 1.437 Å for ^{IV}Al, 1.334 Å for ^{V}Al), and Shannon et al., 1976 (1.328 Å for oxygen associated with ^{VI}Al based on Al-O distance of 1.88 Å). Radii are obtained from simple geometric calculations using published data on typical network cation-oxygen distances and assuming regular polyhedra with the network cation occupying the largest interstices possible while the atoms of oxygen are still 'touching' each other.

To derive the packing fractions, the atomic fraction of each species of network cation per formula unit of a glass (C_{Si}, C_{Al4}, C_{Al5}, C_{Al6}) is first calculated from NMR results. The average volume occupied per oxygen atom is then calculated based on the concentrations of the network cation present in various coordination as per the formula (Zeidler et al, 2014)

$$v_{ox} = \frac{\frac{4}{3}\pi\left[4C_{Si}\, r_{ox}^3 + 4C_{Al[4]}\, r_{ox}^3 + 5C_{Al[5]}\, r_{ox}^3 + 6C_{Al[6]}\, r_{ox}^3\right]}{\left[4C_{Si} + 4C_{Al[4]} + 5C_{Al[5]} + 6C_{Al[6]}\right]} \qquad (1)$$

where the coefficient before the atomic fraction C_{Si}, $C_{Al[4]}$, $C_{Al[5]}$ and $C_{Al[6]}$ is the coordination number for the corresponding cations. The r_{ox} for each cation is given in the paragraph above.

The total volume occupied by oxygen atoms in 1 mole of a given composition of glass (V_{ox}) is obtained from:

$$V_{ox} = v_{ox} . C_O . T_a . N_a \quad (2)$$

where T_a is the total moles of atom per formula unit of glass composition and N_a is Avogadro's number.

V_{ox} was calculated in this manner for each 1 bar and high pressure glass, based on the Al speciation as determined by NMR. The ratios of high pressure to low pressure values help illustrate the response of oxygen anions to compression due to changing Al coordination. It is important to note that this is not an overall response of oxygen to compression but one arising from aluminum structural changes only. Figure 7 plots the volume of oxygen per formula unit normalized to volume of oxygen at 1 bar according to equation 1, versus the relative densification (molar volume decrease, V_0/V) measured by the sink/float method. Here, the values for CAS3010, MAS3010, MAS2020, CAS1525 and CAS2020 are from the current study. A data point for CAS3010 from 5 GPa, as well as results for several high pressure lanthanum, calcium, magnesium, potassium and sodium aluminosilicate glasses are from previous studies (Allwardt et al. 2007; Kelsey et al. 2009a). These spectra were collected with the same 18.8 T spectrometer and methods used here, but were refitted here using DMfit (Massiot et al. 2002) for consistency across all samples. Results and compositions are given in Table 3. Choosing V_0/V as the horizontal axis in Figures 4 and 7, rather than pressure, allows a better assessment

313 of response of the network structure to the actual physical state of the recovered glass, and, in
314 particular, avoids the potential problem of substantial drops in pressure during quench from
315 high temperature liquids in solid-media apparatus, which is likely to have occurred in these
316 earlier studies (Bista et al. 2015). The previously published average Al coordination (obtained by
317 a different fitting method) are somewhat different, but do not change the trends with
318 composition discussed below.

319

320 **DISCUSSION**

321 **Pressure effects on Si and O environments**

322 A number of ^{29}Si NMR studies of alkali silicate glasses, and of alkali aluminosilicates with
323 relatively low Al contents, quenched from initial pressures of 6 to 10 GPa, detected significant
324 populations of ^{V}Si and ^{VI}Si, as well as shifts in ^{IV}Si peaks to higher frequencies that were
325 attributable to decreasing Si-O-Si angles (Xue et al. 1988, 1991; Stebbins and McMillan 1989;
326 Kelsey et al. 2009b). The spectra shown here (Fig. 5) for a low-Al sodium silicate, and for jadeite
327 ($NaAlSi_2O_6$) glass from 2 to 3 GPa from our earlier study (Bista et al. 2015), show that in this
328 lower pressure regime, these kinds of changes are small enough to not be readily observable.
329 In contrast, ^{29}Si spectra for the Ca- and Mg-aluminosilicates do show significant shifts to higher
330 frequencies (less negative chemical shifts) that are correlated with the development of much
331 higher contents of high-coordinated Al. Replacement of Si-O-^{IV}Al with Si-O-^{V}Al linkages should
332 contribute to this effect, as the O-Al bond is expected to become longer and more ionic with
333 increasing Al coordination, possibly resulting in a less negative chemical shift for the

334 neighboring ^{IV}Si (MacKenzie and Smith 2002). The shifts induced by pressure are larger for the
335 peraluminous and metaluminous and smaller for the peralkaline earth Ca-aluminosilicates. This
336 could be caused by competing effects on chemical shifts in the NBO-rich composition. As NBO
337 are consumed at high pressure (Allwardt et al. 2005b), a shift towards more Q^4 species might be
338 expected that would contribute to lowering the mean chemical shift, possibly offsetting some
339 of the other effects of Al coordination increase.

340 ^{27}Al MAS NMR on ^{17}O-enriched CAS2020 and CAS1525 glasses showed increases in Al
341 coordination with pressure that are very similar to those of the unenriched glasses, indicating
342 good experimental control on bulk compositions and P/T paths (Table 2). ^{17}O NMR spectra for
343 both glasses showed similar shifts to higher frequency for the predominant bridging oxygen
344 peak (Fig. 6), which could be related to the development of oxygen linkages to ^{V}Al and ^{VI}Al.
345 However, more specific details of oxygen speciation are difficult to deduce. As previously
346 studied in detail in ambient pressure CAS glasses (Thompson and Stebbins 2011), and as
347 confirmed by these spectra, the NBO content of the peraluminous glass is negligible (<<1%) and
348 that of the metaluminous glass is small (about 2.7%). This emphasizes the need for
349 mechanism(s) not involving NBO for the formation of high coordinated Al at high pressure in
350 such compositions. The shift in the large BO peak with pressure unfortunately obscures
351 pressure effects on the small NBO peak in the CAS2020 glass. However, previous ^{17}O NMR
352 studies of NBO-rich glasses (Lee 2004; Allwardt et al. 2005b; Lee et al. 2012) have clearly shown
353 the reduction in this species with pressure does accompany Al coordination increases.

354

355 **Aluminum coordination, densification, and effects of modifier cation**

356 Previous studies (Allwardt et al. 2004, 2005b; Bista et al. 2015; Gaudio et al. 2015) have
357 highlighted the role of abundant NBO in facilitating Al (and Si) coordination increases with
358 pressure, noting in particular the relatively slow network structural changes in metaluminous
359 compositions such as albite ($NaAlSi_3O_8$) and jadeite ($NaAlSi_2O_6$) (Bista et al. 2015). Data
360 presented here (Table 2, Figs. 3,4) clearly illustrate this effect in the contrasting behavior of
361 CAS3010 and CAS2020, the latter showing significant, but still much smaller increases in ^{V}Al,
362 ^{VI}Al, and mean Al coordination than the former. However, the much greater recovered
363 structural changes in CAS2020 when compared to jadeite, both low in NBO, does suggest an
364 important effect of modifier cation field strength, as has long been noted for NBO-rich
365 compositions as well (Allwardt et al. 2007; Kelsey et al. 2009a).

366 When the modifier cation field strength is further increased from Ca^{2+} to Mg^{2+}, the role
367 of NBO content appears to become dramatically reduced (perhaps because the energetic
368 distinctions among BO and NBO are lessened), as pressure effects on Al speciation for MAS2020
369 and MAS3010 are similar to each other and are well above those in the CAS glasses. Although
370 'anomalous' NBO contents of metaluminous MAS glasses have not been directly measured
371 because of poor chemical shift separation in their ^{17}O NMR spectra, they could be higher than
372 in the CAS system. Nonetheless, the particularly large pressure effects on the MAS2020
373 composition again strongly suggest additional routes to network cation coordination increase
374 that do not involve NBO. And, of course, the large pressure effects on the Al speciation in the
375 peraluminous CAS glass, which should have negligible NBO, supports this conclusion. It is
376 important to note that Al coordination in nominally NBO-free, low modifier field strength

compositions such as albite ($NaAlSi_3O_8$) and rhyolite certainly does increase significantly at pressures above 3 GPa (Allwardt et al. 2005c; Malfait et al. 2012; Gaudio et al. 2015), again requiring 'non-NBO' pathways.

Correlating measured cation coordination changes with recovered glass densification (instead of pressure itself) can provide more insights into structure/property relationships, and also can remove some effects of uncertainty in the final quench pressure. Figure 4 plots our new results for CAS and MAS glasses, for a CAS3010 experiment from 5 GPa (Allwardt et al. 2005a) and for jadeite glass (Bista et al. 2015). For NBO-rich CAS3010 and MAS3010, for a given degree of Al coordination increase, the latter shows a considerably higher densification, suggesting some type of additional structural change is facilitated in the Mg system, possibly a coordination increase in Mg^{2+} itself (Ghosh et al. 2014). Or, in other terms, to reach a given total densification the CAS glass requires a greater change in Al environment than does the MAS glass. In contrast, for the NBO-poor compositions, the MAS2020 curve falls well above that for CAS2020, meaning that Al coordination increase is much greater in the former for a given overall densification. The data for the low-NBO alkali aluminosilicate (jadeite composition) fall even farther below the CAS2020 curve, again emphasizing the dramatic effect of modifier cation field strength ($Na^{1+} < Ca^{2+} < Mg^{2+}$). The close proximity of the curves for MAS3010 and MAS2020 may not be fortuitous, if effectively Mg^{2+} and Al^{3+} are both competing for similar structural roles in 4-, 5- and 6-coordination. Field strength effects have been previously well-documented in high pressure and even in ambient pressure glasses, where Al coordination tends to increase from K- to Na- to Ca- to Mg- to La- aluminosilicate compositions (Allwardt et al. 2007; Kelsey et al. 2009a; Stebbins 2016)

399

400 **Hard sphere model**

401 As described above, Figure 7 plots the calculated change in average oxygen anion
402 volume, caused only by Al coordination increases with pressure, versus the overall
403 densification, and allows comparison of data with a wide range of compositions and an
404 assessment of the roles of different contributions to volume changes. Our new results seem to
405 define relatively narrow range of behavior for most compositions included in this study, as
406 marked by the two dotted lines. For the NBO-rich glasses, CAS3010 follows the upper bound
407 while MAS 3010 follows the lower bound of this band. The NBO-poor glasses, MAS2020 and
408 CAS1525, which have larger concentrations of alumina, follow the upper bound while CAS2020
409 lies in between. Data for jadeite glass, with very little Al coordination increase in this pressure
410 range, appears well outside of this band. Results for several NBO-rich compositions of La-, Ca-,
411 and Mg- aluminosilicates (which have NBO/T and NBO/total oxygen ratios similar to MAS3010)
412 are all close to the lower bound defined by our new results. Three-component Na- and K-
413 aluminosilicates of the same stoichiometry plot in between the two bounds.

414 The upper bound of this band suggests a higher significance of Al coordination increase
415 for the overall densification while the lower bound indicates that the role of aluminum in
416 densification is diluted. The CAS3010 glass follows the upper bound as the presence of
417 significant amounts of NBO promotes Al coordination increase. CAS2020 plots at a lower,
418 intermediate value as the lack of NBO seems to impact the Al coordination increase in this
419 composition. In contrast, for the Mg-aluminosilicate glass, the MAS2020 falls in the upper

bound and MAS3010 falls in the lower bound. As seen in Figure 4, the average Al coordination increase with densification is very similar for both Mg-aluminosilicate glasses probably because there is a mechanism other than NBO consumption: it is possible that both Mg and Al compete for similar role in the Mg-aluminosilicate glasses. The upper bound for MAS2020 and lower bound for MAS3010 in Figure 7 is thus related to the much higher overall alumina concentration of the former.

The LaAS, CMKAS, CMAS glasses, which have NBO-rich compositions analogous to CAS3010 and MAS3010, also fall in the same lower bound as MAS3010. In these, the presence of higher field strength modifier cations (La^{3+}, Mg^{2+}) that can compete with aluminum for strong, short bonds to oxygen (Allwardt et al. 2007; Kelsey et al. 2009a) can again lead to additional pathways for densification, diluting the role of aluminum coordination increase. Direct evidence for increase in the coordination number of La^{3+} with pressure in the LaAS glass was presented previously and supports this suggestion (Kelsey et al. 2009a). Substantial pressure effects on increasing Mg^{2+} and La^{3+} coordination may thus lead to additional densification, and move points to the right (lower bound). Initial compression of the coordination spheres of very "soft" modifier cations such as Na^{+} and K^{+}, which has been noted in effects on ^{23}Na spectra of high pressure glasses (Kelsey et al. 2009b) could have a similar effect. This may change as cation-oxygen distances are reduced at high pressure, possibly effectively increasing the field strength of such modifier cations.

441 **Structural and density relaxation**

442 We conducted high pressure experiments at different temperatures near to the
443 expected T_g, primarily to ensure that temperatures were just high enough to allow relaxation to
444 the metastable equilibrium (supercooled) liquid state. However, these tests also illustrate some
445 of the intriguing issues of relaxation kinetics that have been studied in other systems (Sen et al.
446 2007; Wondraczek et al. 2007, 2009, 2010) and could be the subject of in-depth future studies.
447 Typical results were described in our previous reports (Bista et al. 2015); the complexity of such
448 experiments is illustrated here for Mg-aluminosilicate glasses. For both MAS2020 and
449 MAS3010, the ^{27}Al MAS NMR spectra are slightly different for three samples recovered from
450 three different temperatures at 3 GPa. The highest Al coordination and densification were
451 obtained for both compositions in samples recovered from 835 ˚C, while lower Al coordination
452 and less densification for 810 ˚C samples were probably due to incomplete relaxation. However,
453 the recovered densification and Al coordination were also slightly lower for the glasses from
454 slightly higher temperatures of 855 and 850 ˚C, probably due to the effects of thermal pressure
455 drop during quenching (Bista et al. 2015). For CAS3010, NMR spectra for 3 GPa samples from
456 850 and 810 ˚C were indistinguishable, again indicating structural equilibration at high T and P,
457 but the recovered densities were slightly different, suggesting the possibility of slightly different
458 relaxation kinetics for network cation coordination and overall compaction or decompression.
459 Since we know that only a relatively small fraction of the overall density changes can be directly
460 accounted for by Al coordination increases (Allwardt et al. 2005a; Bista et al. 2015), such a
461 finding could be plausible. However, its novelty and potential importance will require
462 considerable future study to verify.

Implications

One focus of previous studies of pressure-induced structural changes in aluminosilicate glasses has been compositions containing significant NBO and monovalent modifier cations Na^+ and K^+. The contrast of these results with those for well-studied NBO-poor compositions, such as jadeite ($NaAlSi_2O_6$) and albite ($NaAlSi_3O_8$), as well as direct measurements of oxygen speciation by ^{17}O NMR, have shown that NBO can play an important role in aluminum coordination increase with pressure and, therefore, that network speciation change with pressure is more dramatic for depolymerized melts (Lee et al. 2004; Allwardt et al. 2005b; Bista et al. 2015). These conclusions are probably valid for silicic to some intermediate magmas in nature, in which the predominant modifier cations are alkalis and thus have relatively low field strengths. However, they will be overly generalized when considering natural systems that span larger compositional ranges. For example, increased modifier cation field strength is well known to influence network speciation changes, systematically leading to more high coordinated aluminum species (Allwardt et al. 2005a, 2007; Kelsey et al. 2009a). Mafic and ultramafic magmas are dominated by the higher field strength modifiers Mg^{2+}, Ca^{2+}, and Fe^{2+} which can have profound effects on the nature of structural changes with pressure. Our study has thus included Mg- and Ca-rich compositions spanning the range from peralkaline earth, to metaluminous and to peraluminous to reach a broader understanding of the nature of network cation speciation changes with pressure.

Our new results show that the aluminum coordination increase can be equally efficient in both polymerized and depolymerized aluminosilicate glasses when modifier cation field strength is high enough, with especially dramatic findings for magnesium aluminosilicates and intermediate behavior for calcium aluminosilicates. In MAS and CAS systems, pressure effects on metaluminous, nominally fully polymerized compositions are much higher than those in comparable sodium aluminosilicates. These novel results emphasize the important role played by high field strength modifier cations on network structural changes with pressure. In particular, the structures of mafic and ultramafic magmas in nature, which are high in NBO as well as in small, highly charged modifier cations, are likely to be considerably more pressure sensitive than are those of alkali-rich, NBO-poor silicic compositions.

Acknowledgements:

We would like to thank Jodi Puglisi and Corey Liu for access to the 18.8 T spectrometer at the Stanford Magnetic Resonance Laboratory. We thank Thomas W. Sisson and William B. Hankins at the USGS, Menlo Park for support and access to the high pressure apparatus. This work was supported by the NSF, grant EAR-1521055.

References Cited

Allwardt, J.R., Schmidt, B.C., and Stebbins, J.F. (2004) Structural mechanisms of compression and decompression in high-pressure $K_2Si_4O_9$ glasses: an investigation utilizing Raman and NMR spectroscopy of glasses and crystalline materials. Chemical Geology, 213, 137–151.

Allwardt, J.R., Stebbins, J.F., Schmidt, B.C., Frost, D.J., Withers, A.C., and Hirschmann, M.M. (2005a) Aluminum coordination and the densification of high-pressure aluminosilicate glasses. American Mineralogist, 90, 1218–1222.

Allwardt, J.R., Stebbins, J.F., Schmidt, B.C., and Frost, D.J. (2005b) The effect of composition, compression, and decompression on the structure of high-pressure aluminosilicate glasses. An investigation utilizing ^{17}O and ^{27}Al NMR. In Advances in High-Pressure Techniques for Geophysical Applications pp. 211–240. Elsevier.

Allwardt, J.R., Poe, B.T., and Stebbins, J.F. (2005c) The effect of fictive temperature on Al coordination in high-pressure (10 GPa) sodium aluminosilicate glasses. American Mineralogist, 90, 1453–1457.

Allwardt, J.R., Stebbins, J.F., Terasaki, H., Du, L.-S., Frost, D.J., Withers, A.C., Hirschmann, M.M., Suzuki, A., and Ohtani, E. (2007) Effect of structural transitions on properties of high-pressure silicate melts: ^{27}Al NMR, glass densities, and melt viscosities. American Mineralogist, 92, 1093–1104.

Bagdassarov, N.S., Maumus, J., Poe, B., Slutskiy, A.B., and K., B.V. (2004) Pressure Dependence of T g in Silicate Glasses From Electrical Impedance Measurements. Physics and Chemistry of Glasses, 45, 197–214.

Bista, S., O'Donovan-Zavada, A., Mullenbach, T., Franke, M., Affatigato, M., and Feller, S. (2009) Packing in alkali and alkaline earth borosilicate glass systems. Physics and Chemistry of Glasses: European Journal of Glass Science and Technology Part B, 50, 224–228.

Bista, S., Stebbins, J.F., Hankins, W.B., and Sisson, T.W. (2015) Aluminosilicate melts and glasses at 1 to 3 GPa: Temperature and pressure effects on recovered structural and density changes. American Mineralogist, 100, 2298–2307.

Bista, S., Morin, E.I., and Stebbins, J.F. (2016) Response of complex networks to compression: Ca, La, and y aluminoborosilicate glasses formed from liquids at 1 to 3 GPa pressures. Journal of Chemical Physics, 144, 044502.

Brown, G.E., Farges, F., and Calas, G. (1995) X-Ray scattering and X-Ray spectroscopy studiess of silicate melts. In J.F. Stebbins, P.F. McMillan, and D.B. Dingwell, Eds., Reviews in Mineralogy pp. 317–401. Mineralogical Society of America.

Farber, D.L., and Williams, Q. (1996) An in situ Raman spectroscopic study of $Na_2Si_2O_5$ at high pressures and temperatures: Structures of compressed liquids and glasses. American Mineralogist, 81, 273–283.

Gaudio, P. Del, and Behrens, H. (2009) An experimental study on the pressure dependence of viscosity in silicate melts An experimental study on the pressure dependence of viscosity. The Journal of Chemical Physics, 131, 044504.

Gaudio, S.J., Lesher, C.E., Maekawa, H., and Sen, S. (2015) Linking high-pressure structure and density of albite liquid near the glass transition. Geochimica et Cosmochimica Acta, 157, 28–38.

Ghosh, D.B., Karki, B.B., and Stixrude, L. (2014) First-principles molecular dynamics simulations of MgSiO 3 glass : Structure , density , and elasticity at high pressure. American Mineralogist, 99, 1304–1314.

Januchta, K., Youngman, R.E., Goel, A., Bauchy, M., Rzoska, S.J., Bockowski, M., and Smedskjaer, M.M. (2017) Structural origin of high crack resistance in sodium aluminoborate glasses. Journal of Non-Crystalline Solids, 460, 54–65.

Karki, B.B., Bohara, B., and Stixrude, L. (2011) First-principles study of diffusion and viscosity of anorthite ($CaAl_2Si_2O_8$) liquid at high pressure. American Mineralogist, 96, 744–751.

Kelsey, K.E., Stebbins, J.F., Singer, D.M., Brown, G.E., Mosenfelder, J.L., and Asimow, P.D. (2009a) Cation field strength effects on high pressure aluminosilicate glass structure: Multinuclear NMR and La XAFS results. Geochimica et Cosmochimica Acta, 73, 3914–3933.

Kelsey, K.E., Stebbins, J.F., Mosenfelder, J.L., and Asimow, P.D. (2009b) Simultaneous aluminum, silicon, and sodium coordination changes in 6 GPa sodium aluminosilicate glasses. American Mineralogist, 94, 1205–1215.

Lee, S.K. (2003) Order and disorder in sodium silicate glasses and melts at 10 GPa. Geophysical Research Letters, 30, 1845.

——— (2004) Structure of silicate glasses and melts at high pressure: quantum chemical calculations and solid-state NMR. The Journal of Physical Chemistry B, 108, 5889–5900.

Lee, S.K., Cody, G.D., Fei, Y., and Mysen, B.O. (2004) Nature of polymerization and properties of silicate melts and glasses at high pressure. Geochimica et Cosmochimica Acta, 68, 4189–4200.

Lee, S.K., Yi, Y.S., Cody, G.D., Mibe, K., Fei, Y., and Mysen, B.O. (2012) Effect of network polymerization on the pressure-induced structural changes in sodium aluminosilicate glasses and melts: ^{27}Al and ^{17}O solid-state NMR study. Journal of Physical Chemistry C, 116, 2183–2191.

MacKenzie, K., and Smith, M.E. (2002) Multinuclear Solid-State Nuclear Magnetic Resonance of Inorganic Materials. Pergamon.

Malfait, W.J., Verel, R., Ardia, P., and Sanchez-Valle, C. (2012) Aluminum coordination in rhyolite and andesite glasses and melts: Effect of temperature, pressure, composition and water content. Geochimica et Cosmochimica Acta, 77, 11–26.

Malfait, W.J., Seifert, R., and Sanchez-Valle, C. (2014) Densified glasses as structural proxies for high-pressure melts : Configurational compressibility of silicate melts retained in quenched and decompressed glasses. American Mineralogist, 99, 2142–2145.

Massiot, D., Fayon, F., Capron, M., King, I., Le Calvé, S., Alonso, B., Durand, J.-O., Bujoli, B., Gan, Z., and Hoatson, G. (2002) Modelling one- and two-dimensional solid-state NMR spectra. Magnetic Resonance in Chemistry, 40, 70–76.

McMillan, P.F., and Wilding, M.C. (2009) High pressure effects on liquid viscosity and glass transition behaviour, polyamorphic phase transitions and structural properties of glasses and liquids. Journal of Non-Crystalline Solids, 355, 722–732.

Neuville, D.R., Cormier, L., Montouillout, V., Florian, P., Millot, F., Rifflet, J.-C., and Massiot, D. (2008) Amorphous materials: Properties, structure, and durability: Structure of Mg- and Mg/Ca aluminosilicate glasses: ^{27}Al NMR and Raman spectroscopy investigations. American Mineralogist, 93, 1721–1731.

Sen, S., Topping, T., Yu, P., and Youngman, R. (2007) Atomic-scale understanding of structural relaxation in simple and complex borosilicate glasses. Physical Review B, 75, 094203.

Stebbins, J.F. (2016) Glass structure, melt structure, and dynamics: Some concepts for petrology. American Mineralogist, 101, 753–768.

Stebbins, J.F., and McMillan, P.F. (1989) Five- and six-coordinated Si in $K_2Si_4O_9$ glass quenched from 1.9 GPa and 1200'C. American Mineralogist, 74, 965–968.

Stebbins, J.F., Dubinsky, E. V., Kanehashi, K., and Kelsey, K.E. (2008) Temperature effects on non-bridging oxygen and aluminum coordination number in calcium aluminosilicate glasses and melts. Geochimica et Cosmochimica Acta, 72, 910–925.

595 Striepe, S., Smedskjaer, M.M., Deubener, J., Bauer, U., Behrens, H., Potuzak, M., Youngman,
596 R.E., Mauro, J.C., and Yue, Y. (2013) Elastic and micromechanical properties of isostatically
597 compressed soda–lime–borate glasses. Journal of Non-Crystalline Solids, 364, 44–52.

598 Thompson, L.M., and Stebbins, J.F. (2011) Non-bridging oxygen and high-coordinated aluminum
599 in metaluminous and peraluminous calcium and potassium aluminosilicate glasses: High-
600 resolution ^{17}O and ^{27}Al MAS NMR results. American Mineralogist, 96, 841–853.

601 Wang, Y., Sakamaki, T., Skinner, L.B., Jing, Z., Yu, T., Kono, Y., Park, C., Shen, G., Rivers, M.L., and
602 Sutton, S.R. (2014) Atomistic insight into viscosity and density of silicate melts under
603 pressure. Nature Communications, 5, 3241.

604 Wolf, G.H., Durben, D.J., and McMillan, P.F. (1990) High-pressure Raman spectroscopic study of
605 sodium tetrasilicate ($Na_2Si_4O_9$) glass. The Journal of Chemical Physics, 93, 2280.

606 Wondraczek, L., Behrens, H., Yue, Y., Deubener, J., and Scherer, G.W. (2007) Relaxation and
607 glass transition in an isostatically compressed diopside glass. Journal of the American
608 Ceramic Society, 90, 1556–1561.

609 Wondraczek, L., Krolikowski, S., Behrens, H., Wondraczek, L., Krolikowski, S., and Behrens, H.
610 (2009) Relaxation and Prigogine – Defay ratio of compressed glasses with negative
611 viscosity- pressure dependence. Journal of Chemical Physics, 130, 204506.

612 Wondraczek, L., Krolikowski, S., and Behrens, H. (2010) Kinetics of pressure relaxation in a
613 compressed alkali borosilicate glass. Journal of Non-Crystalline Solids, 356, 1859–1862.

614 Xue, X., Stebbins, J.F., Kanzaki, M., and Tronnes, R.G. (1988) Silicon coordination and speciation
615 changes in a silicate liquid at high pressures. Science, 699, 1987–1990.

616 Xue, X., Stebbins, J.F., Kanzaki, M., McMillan, P.F., and Poe, B. (1991) Pressure-induced silicon
617 coordination and tetrahedral structural changes in alkali oxide-silica melts up to 12 GPa:
618 NMR, Raman, and infrared spectroscopy. American Mineralogist, 76, 8–26.

619 Yarger, J.L., Smith, K.H., Nieman, R.A., Diefenbacher, J., Wolf, G.H., Poe, B.T., and McMillan, P.F.
620 (1995) Al coordination changes in high-pressure aluminosilicate liquids. Science.

621 Zeidler, A., Salmon, P.S., and Skinner, L.B. (2014) Packing and the structural transformations in
622 liquid and amorphous oxides from ambient to extreme conditions. Proceedings of the
623 National Academy of Sciences, 111, 10045–10048.

624

625

626 Table 1: Compositional analyses from electron microprobe, in mol%

Sample	**CaO**	**MgO**	**Al_2O_3**	**SiO_2**
CAS 3010	30.3		9.9	59.8
CAS 2020	20.4		19.9	59.7
CAS 1525	15.3		24.6	60
MAS 3010		30	9.9	60.1
MAS 2020		20.2	19.7	60

627 Error range estimated at ±0.5 mol%

628

Table 2: Experimental conditions, ambient pressure glass transition temperatures (T_g), Al speciation, and relative densities

Sample	1 bar Tg (°C)	P (GPa)	T (°C)	^{IV}Al	^{V}Al	^{VI}Al	Average Al CN (±0.02)	Relative density	density
CAS 3010	783	1 bar		0.97	.03		4.03		2.7
CAS 3010		1	850	.93	.07		4.07	1.022(1)	2.75
CAS 3010		2	850	.79	.19	.02	4.23	1.052(1)	2.85
CAS 3010[a]		3	850	.64	.29	.07	4.43	1.082(2)	2.91
CAS 3010		3	810	.64	.29	.07	4.43	1.074(2)	
CAS 3010[b]		5		.47	.37	.16	4.69	1.107	
CAS 2020	862	1 bar		.96	.04	0	4.04		2.62
CAS 2020		3	810	.75	.21	.03	4.23	1.096(1)	2.87
CAS 2020[c]		1 bar		.97	.03		4.03		
CAS 2020[c]		3		.77	.20	.03	4.26		
CAS 1525	865	1 bar		0.9	0.1	0	4.1		2.62
CAS 1525		3	865	0.62	0.3	0.07	4.4	1.113(1)	2.92
CAS 1525		3	845	0.62	0.3	0.07	4.4		
CAS 1525[c]		1 bar		.88	.12		4.12		
CAS 1525[c]		3		.65	.3	.05	4.4		
MAS 3010	785	1 bar		97	.03	0	4.03		2.6
MAS 3010		1.5	790	.87	.1	.03	4.16	1.051(1)	2.74
MAS 3010		3	835	.59	.31	.1	4.51	1.118(1)	2.9
MAS 3010		3	810	.62	.30	.08	4.46	1.108(1)	
MAS 3010		3	855	.64	.29	.07	4.39	1.105(1)	
MAS 2020	810	1 bar		.94	.05	0	4.01		2.59
MAS 2020		1.5	815	.82	.15	.03	4.21	1.058(1)	2.74
MAS 2020		3	835	.57	.33	.1	4.53	1.128(1)	2.92
MAS 2020		3	810	.60	.31	.09	4.43	1.120(1)	
MAS 2020		3	850	.59	.31	.1	4.50	1.126(1)	

Error on absolute density measurement based on known standards is estimated to be ±0.02 g/cm^3.
Error on relative density measurement based on the error propagation of the 1σ value of absolute density.
Error on average aluminum coordination based on the error propagation of the 1σ value of different al species

[a]values from Bista et al., 2015

[b]values obtained by refitting spectra from Allwardt et al., 2007

638 ᶜO17 enriched samples with values for 1 bar obtained from Thompson et al, 2011 and 3 GPa values
639 were obtained from high pressure experiments on O17 enriched sample in current study

640

641 Table 3: Al speciation obtained from the refitting of ^{27}Al spectra from previous studies using the Czjzek
642 distribution of the quadrupolar coupling parameter in DMFIT (Massiot et al. 2002).

Sample	Composition (mol%)						Pressure (GPa)	^{IV}Al	^{V}Al	^{VI}Al
	K_2O	CaO	MgO	La_2O_3	Al_2O_3	SiO_2				
CMKAS[a]	5	17.5	7.5		10	60	0.0001	98	2	0
CMKAS[a]	5	17.5	7.5		10	60	3	88	10	2
CMKAS[a]	5	17.5	7.5		10	60	8	41	39	20
CMKAS[a]	5	17.5	7.5		10	60	10	42	40	18
CMAS[a]		15	15		10	60	0.0001	99	1	0
CMAS[a]		15	15		10	60	3	78	18	4
C2KAS[a]	20	10			10	60	0.0001			
C2KAS[a]	20	10			10	60	3	92	7	1
C2KAS[a]	20	10			10	60	5	74	21	5
C2KAS[a]	20	10			10	60	8	47	38	15
LaAS[b]				12.5	12.5	75	0.0001	95	3	2
LaAS[b]				12.5	12.5	75	6	44	39	17
CAS[c]		30			10	60	0.0001	97	3	
CAS[a]		30			10	60	5	47	37	16
CAS[a]		30			10	60	8	31	45	24

643 The NBO/TO ~ 0.17 and NBO/T ~ 0.37 in all the compositions listed in the table above.

644 [a]Allwardt et al., 2007

645 [b]Kelsey et al., 2009b

646 [c]Bista et al., 2015

647

648

Figure captions

Figure 1: Overlay of ^{27}Al MAS NMR spectra of glasses recovered from various pressures as labeled. **(a)** metaluminous (CAS2020) glass. **(b)** peraluminous (CAS1525) glass. **(c)** metaluminous (MAS2020) glass. **(d)** peralkaline-earth (MAS3010) glass.

Figure 2: ^{27}Al MAS NMR spectra of glasses recovered from 3 GPa and different temperature for confirming structural relaxation. **(a)** Above: CAS3010 glass recovered from 3 GPa and 810 °C (solid), 850 °C (dotted). Below: CAS1525 glass recovered from 3 GPa and 845 °C (solid) 865 °C (dotted). **(b)** Above: MAS3010 glass recovered from 3 GPa and, 835 °C (dashed), 810 °C (solid) and 855 °C (dotted). Below: MAS2020 glass recovered from 3 GPa and 835 °C (dashed), 810 °C (solid) and 850 °C (dotted).

Figure 3: Average Al coordination versus pressure for Ca- and Mg-aluminosilicate glasses in the current study, and for jadeite ($NaAlSi_2O_6$) glass (Bista, et al. 2015).

Figure 4: Average Al coordination versus densification for Ca- and Mg-aluminosilicate glasses in the current study, and for jadeite ($NaAlSi_2O_6$) glass (Bista, et al. 2015).

Figure 5: ^{29}Si MAS NMR spectra of jadeite, NS3 ($Na_2Si_3O_7$), CAS1525, CAS2020 and CAS3010 (bottom) glasses recovered from 1 bar (solid), 3 GPa (dashed) and 2 GPa (dashed for NS3).

Figure 6: ^{17}O MAS NMR spectra overlay of CAS1525 and CAS2020 glasses recovered from 1 bar (solid) and 3 GPa (dashed).

Figure 7: Relative densification of oxygen anion due to aluminum coordination derived from ^{27}Al MAS NMR data (y-axis) versus overall densification of glass obtained from sink/float technique (x axis).

670

671

672

673

674

675

This is a preprint, the final version is subject to change, of the American Mineralogist (MSA)
Cite as Authors (Year) Title. American Mineralogist, in press.
(DOI will not work until issue is live.) DOI: http://dx.doi.org/10.2138/am-2017-6081

Figure 1a:

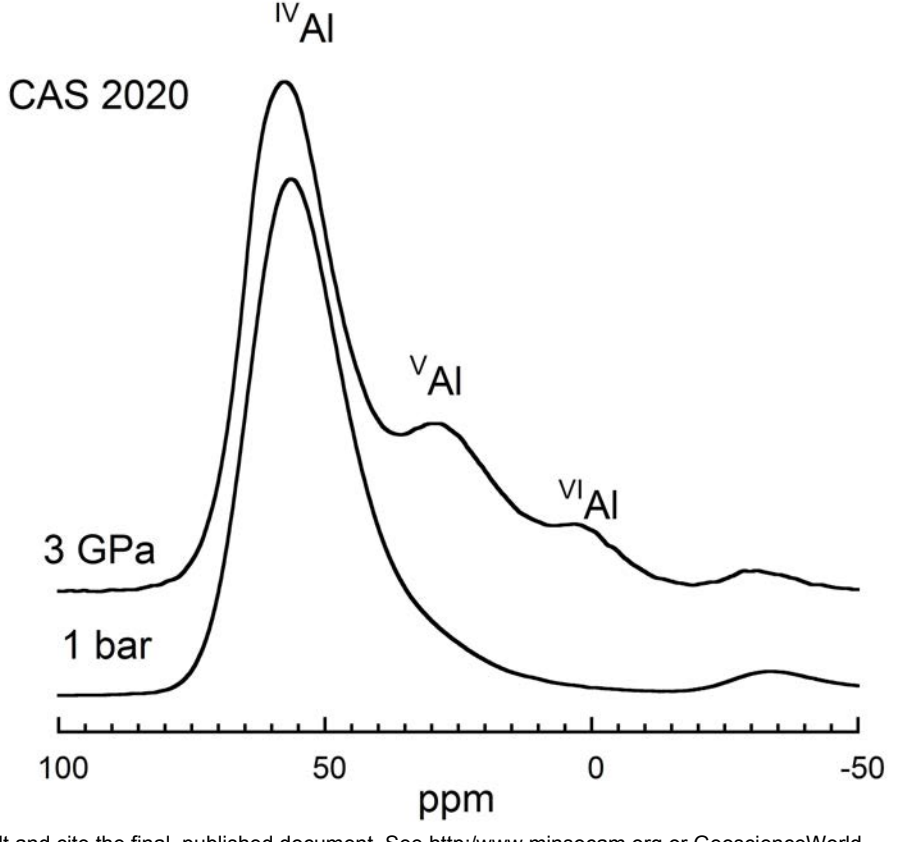

This is a preprint, the final version is subject to change, of the American Mineralogist (MSA)
Cite as Authors (Year) Title. American Mineralogist, in press.
(DOI will not work until issue is live.) DOI: http://dx.doi.org/10.2138/am-2017-6081

Figure 1b:

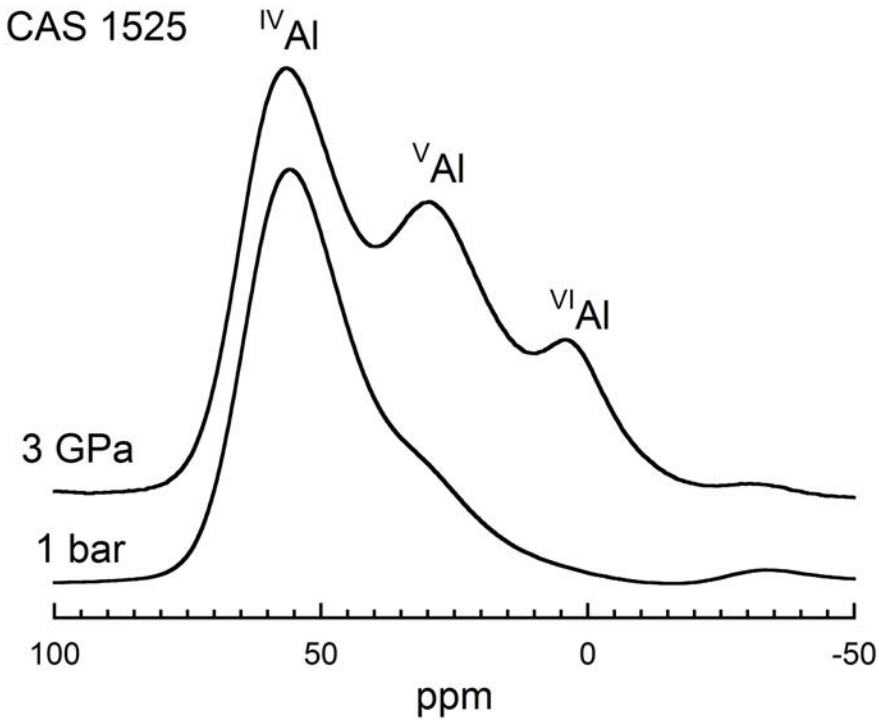

This is a preprint, the final version is subject to change, of the American Mineralogist (MSA)
Cite as Authors (Year) Title. American Mineralogist, in press.
(DOI will not work until issue is live.) DOI: http://dx.doi.org/10.2138/am-2017-6081

Figure 1c:

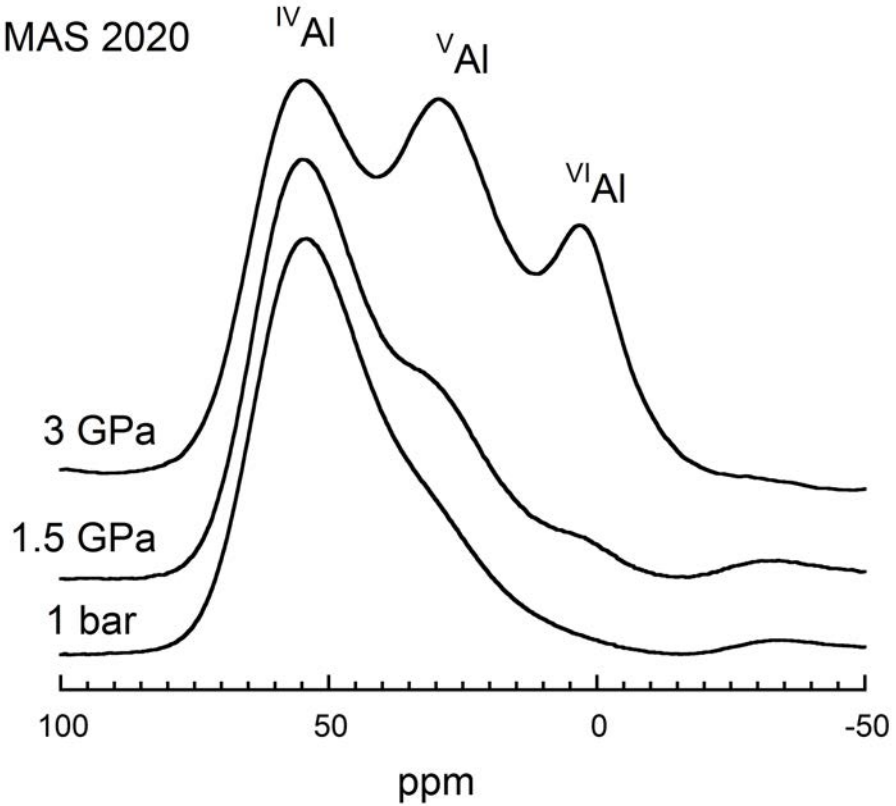

This is a preprint, the final version is subject to change, of the American Mineralogist (MSA)
Cite as Authors (Year) Title. American Mineralogist, in press.
(DOI will not work until issue is live.) DOI: http://dx.doi.org/10.2138/am-2017-6081

Figure 1d

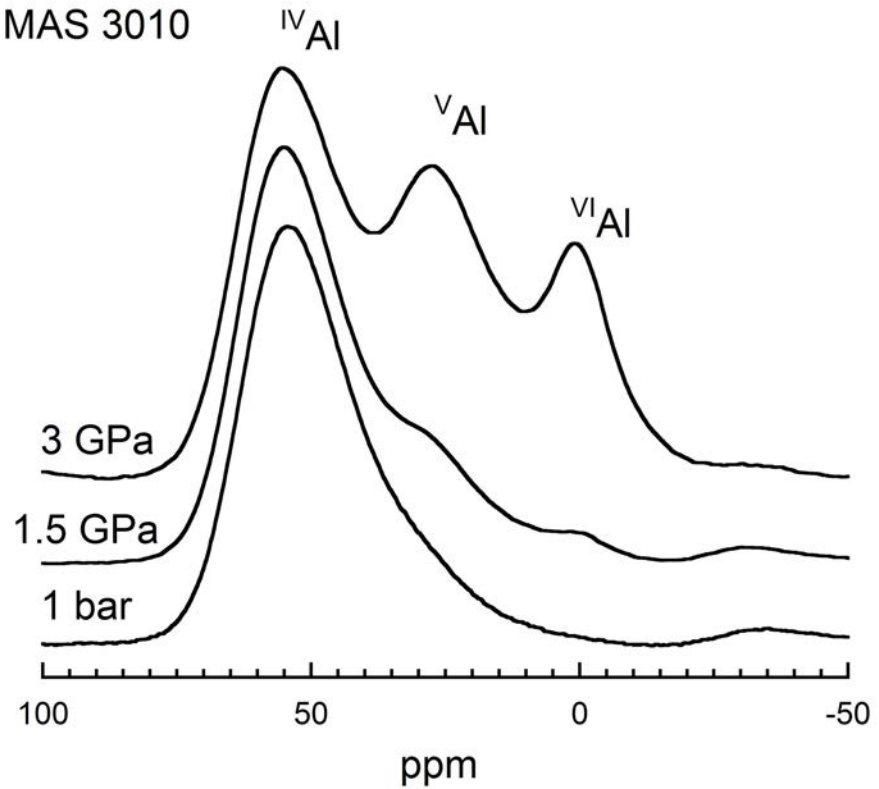

This is a preprint, the final version is subject to change, of the American Mineralogist (MSA)
Cite as Authors (Year) Title. American Mineralogist, in press.
(DOI will not work until issue is live.) DOI: http://dx.doi.org/10.2138/am-2017-6081

Figure 2a:

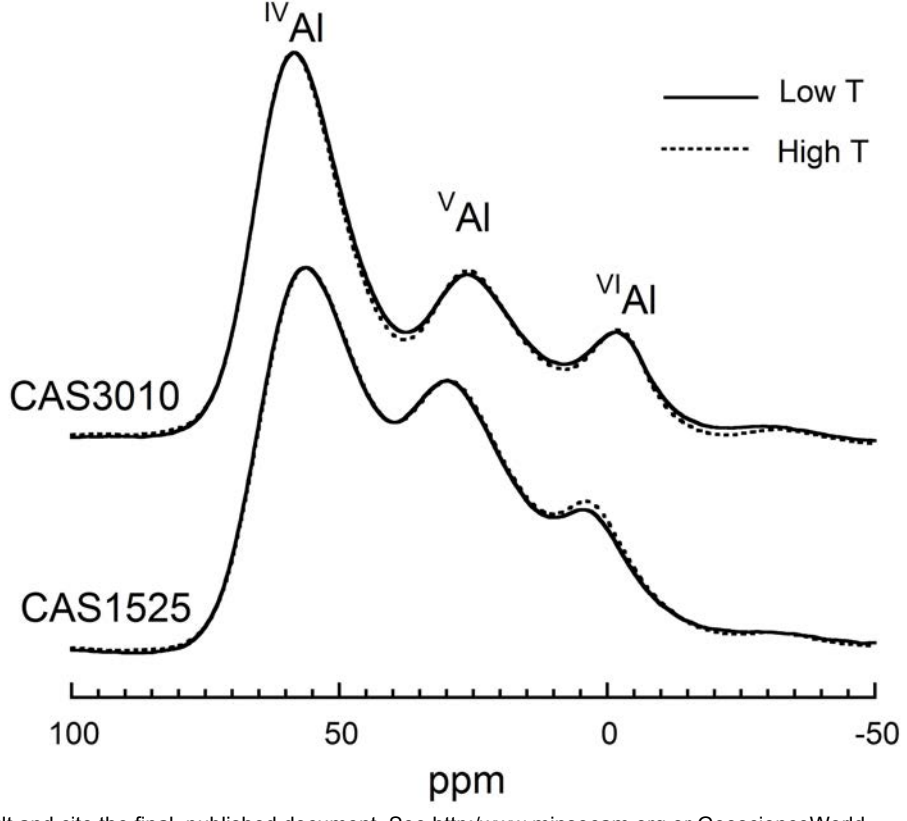

This is a preprint, the final version is subject to change, of the American Mineralogist (MSA)
Cite as Authors (Year) Title. American Mineralogist, in press.
(DOI will not work until issue is live.) DOI: http://dx.doi.org/10.2138/am-2017-6081

Figure 2b:

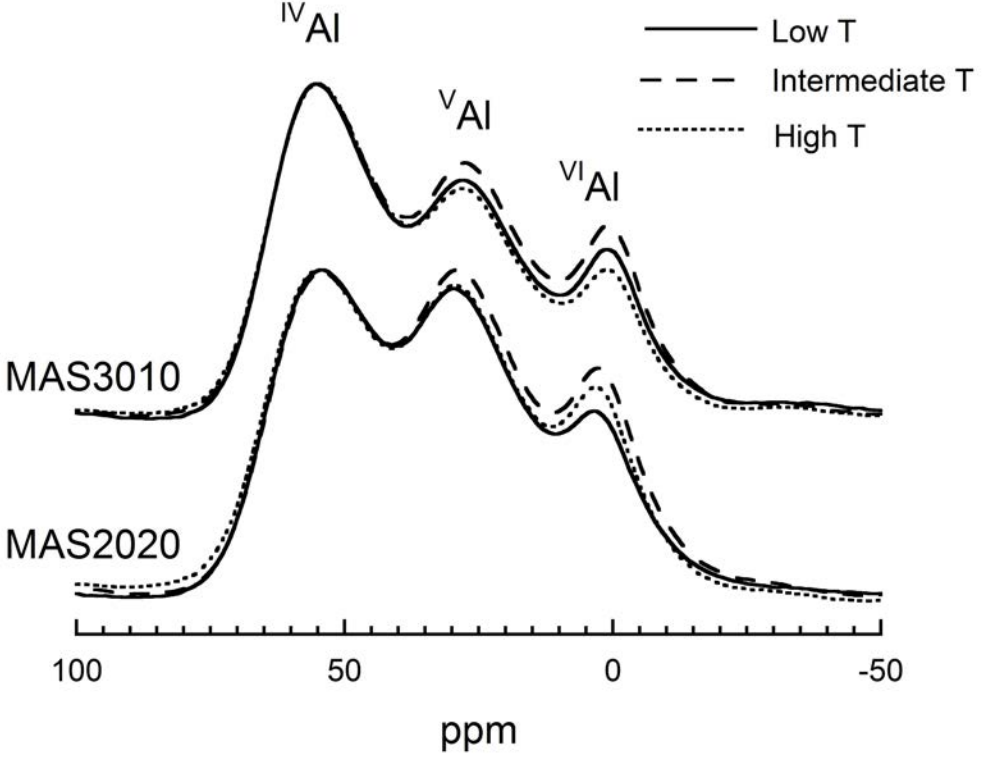

This is a preprint, the final version is subject to change, of the American Mineralogist (MSA)
Cite as Authors (Year) Title. American Mineralogist, in press.
(DOI will not work until issue is live.) DOI: http://dx.doi.org/10.2138/am-2017-6081

Figure 3:

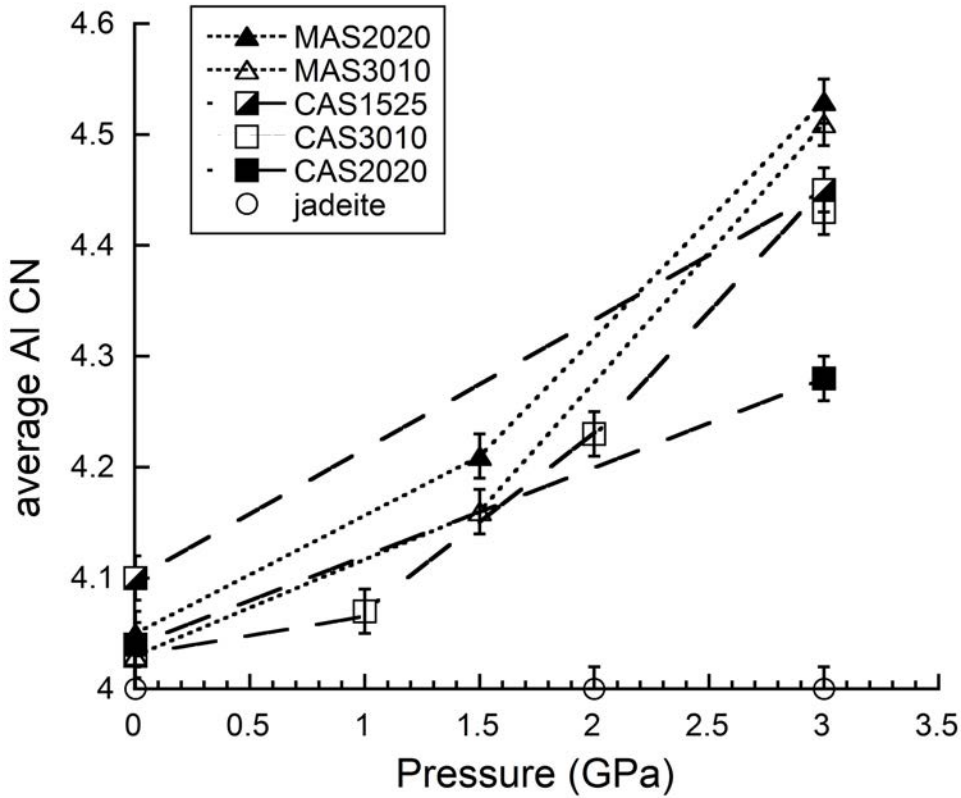

This is a preprint, the final version is subject to change, of the American Mineralogist (MSA)
Cite as Authors (Year) Title. American Mineralogist, in press.
(DOI will not work until issue is live.) DOI: http://dx.doi.org/10.2138/am-2017-6081

Figure 4:

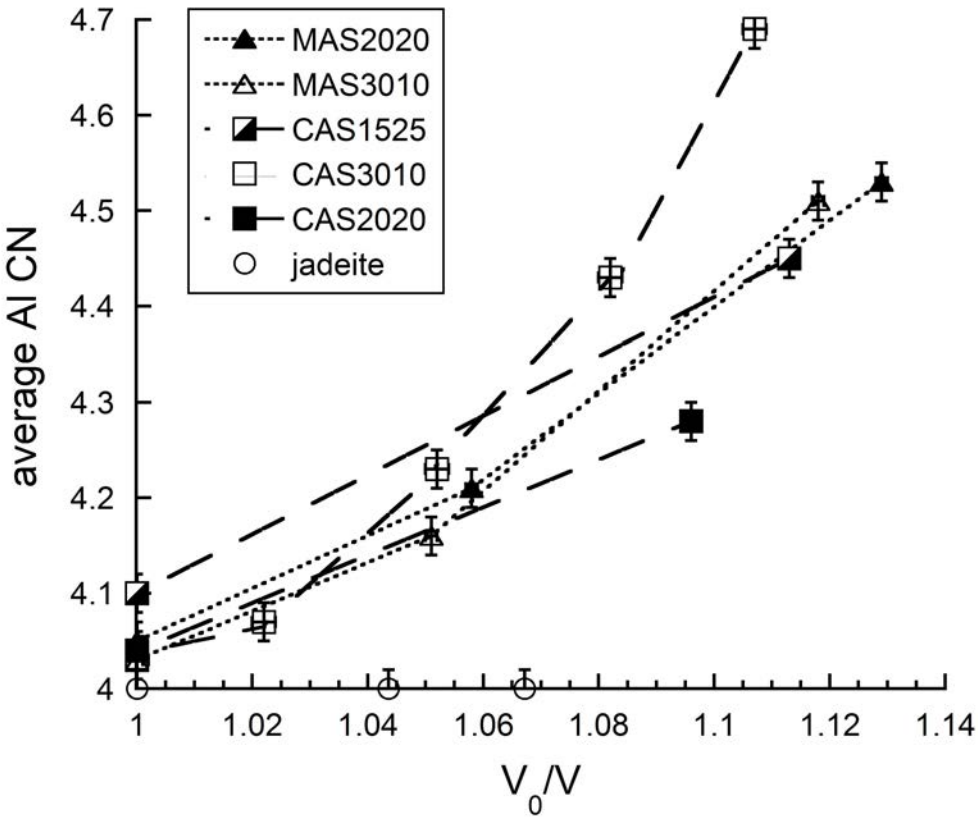

This is a preprint, the final version is subject to change, of the American Mineralogist (MSA)
Cite as Authors (Year) Title. American Mineralogist, in press.
(DOI will not work until issue is live.) DOI: http://dx.doi.org/10.2138/am-2017-6081

Figure 5:

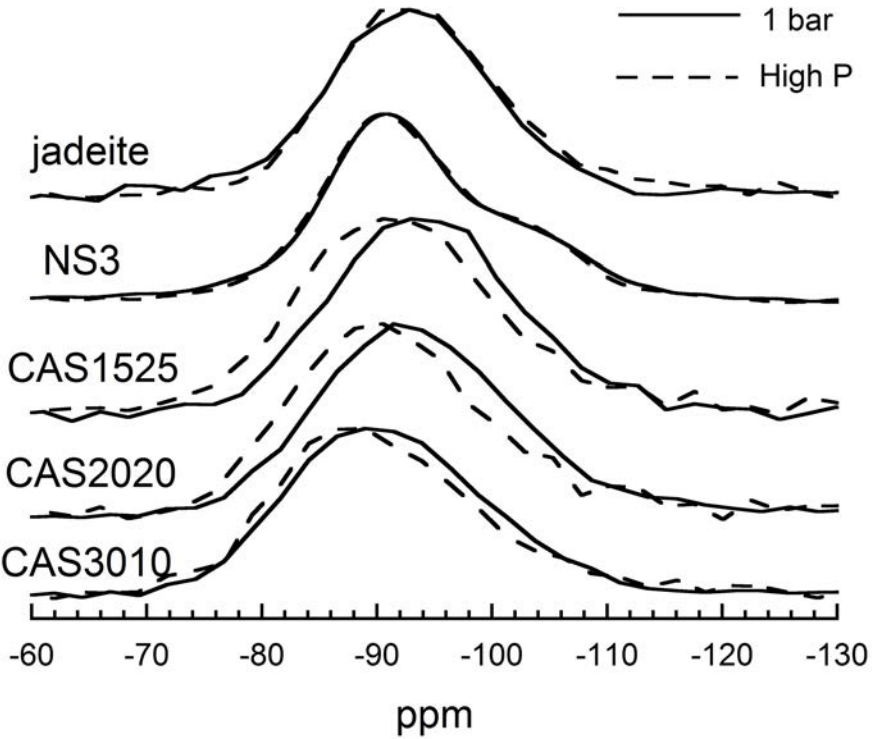

This is a preprint, the final version is subject to change, of the American Mineralogist (MSA)
Cite as Authors (Year) Title. American Mineralogist, in press.
(DOI will not work until issue is live.) DOI: http://dx.doi.org/10.2138/am-2017-6081

Figure 6:

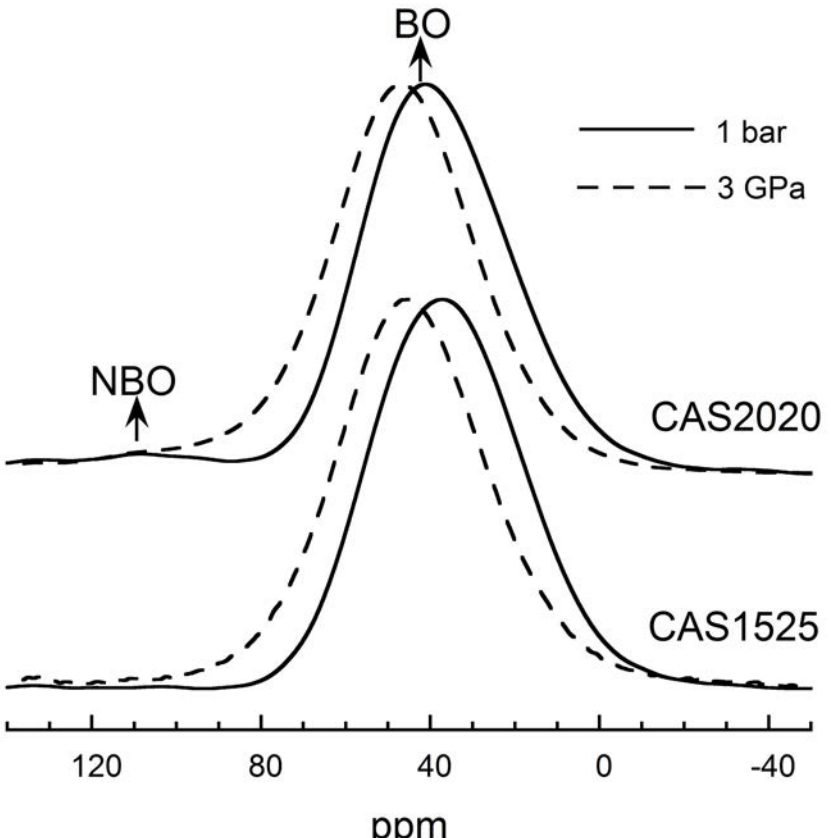

This is a preprint, the final version is subject to change, of the American Mineralogist (MSA)
Cite as Authors (Year) Title. American Mineralogist, in press.
(DOI will not work until issue is live.) DOI: http://dx.doi.org/10.2138/am-2017-6081

Figure 7